Fermiology of Cr and Mo

1998 J. Phys.: Condens. Matter 10 10367

(http://iopscience.iop.org/0953-8984/10/46/003)

J. Phys.: Condens. Matter **10** (1998) 10367–10374. Printed in the UK PII: S0953-8984(98)97352-0

Fermiology of Cr and Mo

S B Dugdale†‡, H M Fretwell†, D C R Hedley†, M A Alam†, T Jarlborg‡, G Santi‡, R M Singru§†, V Sundararajan‖ and M J Cooper¶

† H H Wills Physics Laboratory, University of Bristol, Tyndall Avenue, Bristol BS8 1TL, UK

‡ Département de Physique de la Matière Condensée, Université de Genève, 24 quai Ernest Ansermet, CH-1211 Genève 4, Switzerland

§ Indian Institute of Technology, Department of Physics, Kanpur 208016, Uttar Pradesh, India

‖ Centre for Development of Advanced Computing, Pune University Campus, Pune 411 007, India

¶ Department of Physics, University of Warwick, Coventry CV4 7AL, UK

Received 30 April 1998

Abstract. An interpretation of the two-dimensional angular correlation of positron annihilation radiation (2D-ACAR) for paramagnetic chromium (Cr) and molybdenum (Mo) is presented. Rather than explaining the significant differences in the resulting $\boldsymbol{k}$-space occupancies in terms of different Fermi surface (FS) topologies, the recovery of a FS topology for paramagnetic Cr in agreement with band theory (and similar to the Mo experiment) through the application of a recently introduced maximum-entropy-based filtering technique suggests an explanation related to positron wavefunction perturbations.

1. Introduction

The electronic structure of chromium (Cr), among the 3d transition metals, remains an interesting subject, not least because of its unusual magnetic behaviour [1]. Above ∼311 K, Cr is paramagnetic, and thus any study using the traditional quantum oscillatory fermiological tools is necessarily precluded. However, a variety of band theoretical computations predict a Fermi surface (FS) topology which is similar to that of Mo, its isoelectronic counterpart. In recent years, a number of positron annihilation experiments have produced a FS picture which, although containing some similar features, is still significantly different from that of Mo. We highlight differences in the momentum densities and associated FS topologies of paramagnetic Cr and Mo as measured in our recent positron experiments. And, in the light of new data analysis techniques, we point out that the apparent discrepancies may arise from different behaviours of the positron in these metals, rather than from different FS topologies.

The positron annihilation technique relies only on the conservation of momentum and energy, and unlike the quantum oscillatory techniques, is not restricted to just low-temperature fermiology. Positrons probe the occupied electronic states in reciprocal space via measurements of the angular deviations (from anticollinearity) between the pair of annihilation γ-photons [2]. A two-dimensional angular correlation of positron annihilation radiation (2D-ACAR) experiment yields a 2D projection (or integral over one dimension), $N(p_x, p_y)$, of the underlying electron–positron momentum density, $\rho^{2\gamma}(\boldsymbol{p})$:

$$N(p_x, p_y) = \int_{-\infty}^{\infty} \rho^{2\gamma}(\boldsymbol{p})\ \mathrm{d}p_z \tag{1}$$

0953-8984/98/4610367+08$19.50

where

$$\rho^{2\gamma}(\boldsymbol{p}) = \sum_j n_j(\boldsymbol{k}) \left| \int \exp[-\mathrm{i}\boldsymbol{p}\cdot\boldsymbol{r}]\psi_j(\boldsymbol{r})\psi_+(\boldsymbol{r})\ \mathrm{d}\boldsymbol{r} \right|^2 \tag{2}$$

with $n_j(\boldsymbol{k})$ representing the electron occupancy in $\boldsymbol{k}$-space associated with band j. Within the independent-particle model (IPM), equation (2) describes the electron–positron (or two-photon) momentum density, which contains all of the information about the electron and positron wavefunctions, $\psi_j(\boldsymbol{r})$ and $\psi_+(\boldsymbol{r})$ respectively. Also, equation (2) indicates that $\rho^{2\gamma}(\boldsymbol{p})$ will exhibit a discontinuity when a partially occupied band crosses the Fermi energy. The momentum density has the full point symmetry of the crystalline lattice, and the translational invariance can be restored through the application of the Lock–Crisp–West prescription [3], which gives the occupancy in $\boldsymbol{k}$-space, $n(\boldsymbol{k})$, by 'folding' the equivalent points in the momentum density back into the first Brillouin zone (BZ). If the effects of the positron wavefunction can be ignored (or more specifically, if the positron wavefunction is $\boldsymbol{k}$-independent), then this latter image will depend only on the electron occupancy in momentum space, allowing (a projection of) the FS topology to be inferred.

The success of the positron technique in revealing the FS topologies of simple metals, transition metals and transition metal alloys has been amply demonstrated [2]. Although the LCW theorem is only valid in the case of a constant ($\boldsymbol{k}$-independent) positron wavefunction, these experiments have shown that the perturbations introduced are generally small enough not to mask the FS-related effects. Projection-dependent perturbations have been considered by Lock and West [4], where the LCW distributions from 1D-ACAR experiments on Cu along two different directions were considered. In one direction, [110], the distribution closely reflected the FS topology, but in the other ([100]), the distribution was heavily affected by the positron wavefunction. More recently, 2D-ACAR experiments have been performed on complex high-T_C superconductors and heavy-fermion systems [2]. Here, however, the extraction of FS information has not been without difficulty. In these materials, the FS signals are weak due to a smaller number of partially occupied bands compared to the total number of bands contributing to the annihilation process. In addition, the unit cells are large, leading to small BZs only a few times larger than the experimental resolution.

In such systems, it has been proposed that a $\boldsymbol{k}$-dependent positron wavefunction modulates the underlying electron occupancy to such an extent that the Fermi breaks are not readily observable [5, 6]. The recent introduction of filters by the current authors [7] and others [8, 9] to retrieve the FS illustrates that 2D-ACAR can be used in studying the fermiology of these materials. While the possibility of stronger wavefunction perturbations in more complicated, multiple-basis systems (such as in the high-T_C superconductors and heavy-fermion systems) might be expected due to the more anisotropic positron 'density' within the unit cell, such effects in a transition metal would be surprising. However, in view of the significantly different FS picture (compared to those for Mo and band theory) for paramagnetic Cr revealed in the positron annihilation data, the appearance of just such a situation may not be discounted. Therefore, we applied the same FS retrieval procedure as was mentioned above to positron data for Cr and Mo and discuss the resulting features in order to better understand the positron results.

Lomer (see [10]) was the first to propose a FS for BCC Cr; it was based on a band-structure calculation for iron by Wood [11] (see figure 1). Previous 2D-ACAR studies of Mo [12] have revealed a FS topology in close agreement with the theoretical predictions. Conversely, as mentioned earlier, 2D-ACAR experiments performed on paramagnetic Cr have always yielded a somewhat different FS topology from both that from theoretical calculations [13–16] and that of Mo. It is common practice, when attempting to compare

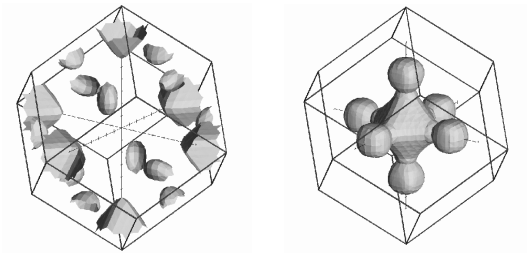

Figure 1. The Fermi surface of the Cr from the LMTO calculation. Left: holes in band 3. Right: electrons in band 4. The electron lenses in band 5 are ignored as they are too small to be observed in a 2D-ACAR experiment.

experimental data with calculations, to convolute the theoretical results with some function representing the experimental resolution. Matsumoto and Wakoh [14], in order to bring their theoretical data into reasonable agreement with experiment, had to convolute their distributions with a function two to three times broader than the actual experimental resolution.

Before beginning a comparison of the various data sets, the techniques employed to extract the FS topology for the more complex system referred to earlier need to be briefly elaborated upon. The essential element of the Bristol [7] and Arlington [9] schemes is edge enhancement. The Arlington scheme is effectively a 'band-pass' filter, strengthening the FS-related discontinuities (high frequency) while suppressing the lower-frequency variations. Here, the data are smoothed, before this smoothed version of the data is subtracted from the raw data. After applying a final smoothing (to suppress the noise level that has necessarily increased during the subtraction process), the final spectrum should contain stronger FS-related features. The Bristol scheme also has its origins in the field of image processing and is based upon a maximum-entropy deconvolution scheme [17]. Although originally developed to carefully remove the unwanted convolution with the experimental resolution in 2D-ACAR spectra without introducing noise or artefacts, its potential for revealing the FS topology was also exploited. Since the greatest effect of the convolution with the experimental resolution is likely to be around the FS-related discontinuities, a 'raw' distribution subtracted from a deconvoluted distribution ought to reveal FS features in this 'difference' spectrum. The results of the application of this algorithm to vanadium data were presented in [7]. Subsequently, this and other techniques have successfully revealed the normal-state FS of the heavy-fermion compound CeB_6 [6]. The similarity of the two approaches should be emphasized (one smoothing the data and subtracting it from the raw data, one deconvoluting the data and then subtracting the raw data), and have been shown to generate almost identical results [6].

2. Experimental details

The current 2D-ACAR data were measured on the Bristol 2D-ACAR machine. The details of this type of spectrometer can be found elsewhere [18]. Normally, in order to optimize resolution, ACAR experiments are performed at as low a temperature as possible. The Cr data were collected at 353 K, more than 40 K above the Néel temperature, because studies have shown (private communication in [13]) that residual strains within the sample can sustain the existence of the AFM phase. However, at 353 K, the sample can be considered completely paramagnetic.

All of the data sets contained in excess of 220 million counts, and were treated in the same manner before finally applying the LCW prescription to generate $\boldsymbol{k}$-space densities. For comparison, the electron momentum densities were calculated using two different methods; both the LMTO (linearized muffin-tin orbital) [19] and LCGO [15] (linear combination of Gaussian orbitals) were employed, within the local density approximation. The FS topologies generated by the two methods were essentially identical to each other (and to those from previous calculations), and for brevity, here we present only the LMTO results (figure 1). The electron occupancies were constructed both from the LCW folding of the momentum density and from the energy bands, to make sure that sufficient $\boldsymbol{G}$-vectors were included. It should be borne in mind that the theoretical results have not been convoluted to simulate the effect of the experimental resolution.

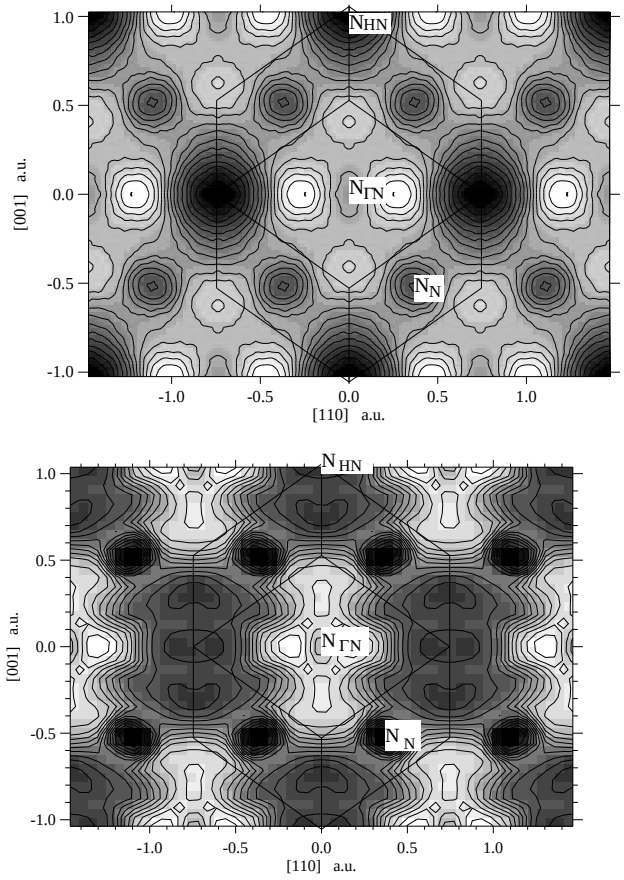

Figure 2. The LCW distribution of Mo [110]: experiment (top) and LMTO theory (bottom). In all of the figures, the white areas represent high electron density (i.e. electrons) and the black areas, low electron density (i.e. holes).

3. Results

The results are presented in figures 2–5. In all of the figures, the dark areas represent unoccupied states (hole FS features) and the white areas are occupied regions (electron

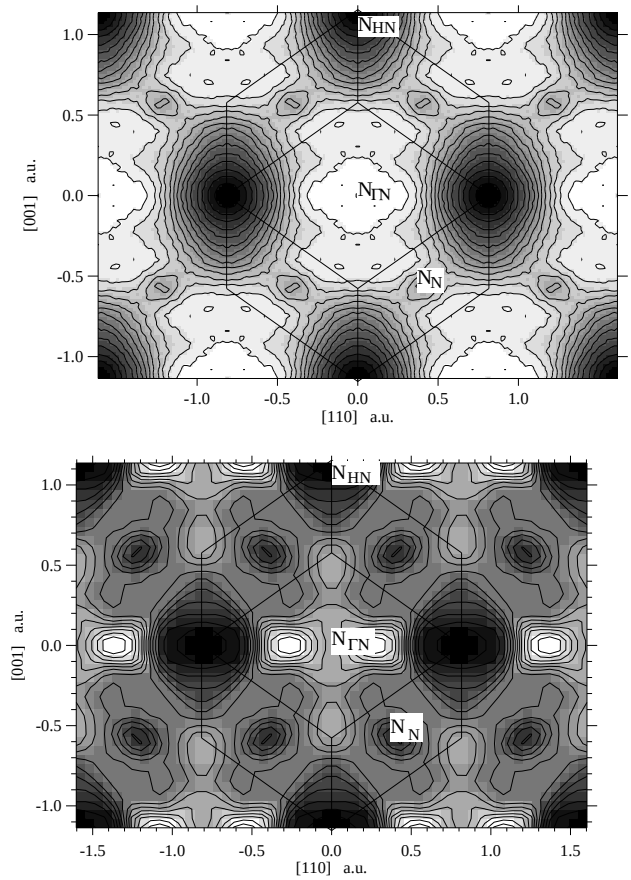

Figure 3. The LCW distribution of Cr [110]: experiment (top) and LMTO theory.

FS features). The LCW distributions for Mo at the two temperatures exhibit the expected FS features such as the N-centred hole pockets (which are very prominent as they project directly onto other N points), and the knobs of the electron jack. Indeed, the two knobs along the [110] direction show up as much 'whiter' compared with the two along [100], as one would expect after considering the projection through the BZ and the resulting superposition of *two* knobs on each of these points. The H-hole octahedra are also distinguishable. Measurements made on Mo at ∼30 K (figure 2) and at room temperature (not shown) were almost indistinguishable except for thermal broadening (the momentum resolution in an ACAR experiment is degraded at room temperature by the increased positron thermal energy).

In figures 3 and 4, the Cr data are presented for two projection directions alongside the respective LMTO theoretical distributions. In comparison with the Mo data, the degree of agreement with the Lomer picture [10], and more significantly with the current theoretical predictions, is less satisfactory for Cr. The size of the N-hole pockets is different, and the knobs on the electron jack are not visible. In figure 5, the LCW distributions from the 'maximum-entropy'-processed data are presented for the [100] and [110] projections respectively. Now a FS topology similar to that of the theory (and of Mo) is apparent. The current observations cannot be attributed to the particular sample, as previous experiments

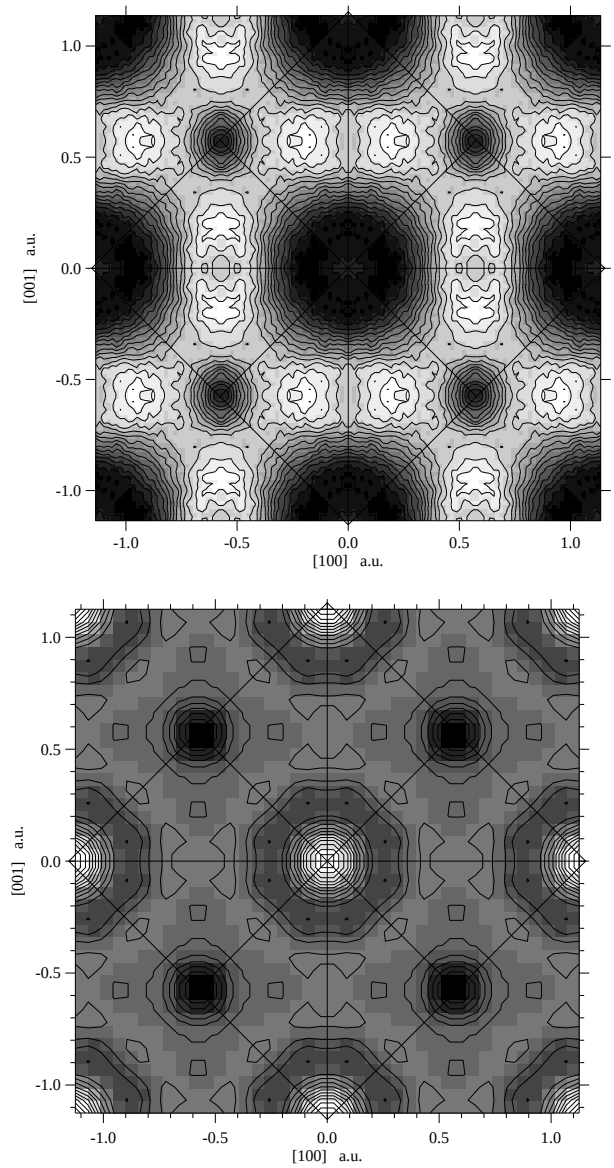

Figure 4. The LCW distribution of Cr [100]: experiment (top) and LMTO theory.

performed on different specimens and in different laboratories [13, 16] have produced similar results. Positron lifetime measurements on the sample produced a single-component spectrum, indicating that the sample was free of defects.

In view of the clear discrepancy between theory and experiment in the case of Cr, two possibilities present themselves: either the electronic structure of Cr is different from that predicted by a self-consistent band calculation, with a different FS topology from Mo, or the positron-induced perturbations are so much stronger in Cr (with respect to Mo) that these dominate the FS signatures present in $\rho^{2\gamma}(\boldsymbol{p})$. The recovery of an electron $\boldsymbol{k}$-space occupancy in Cr that is similar to that in Mo (and that of theory) through the maximum-

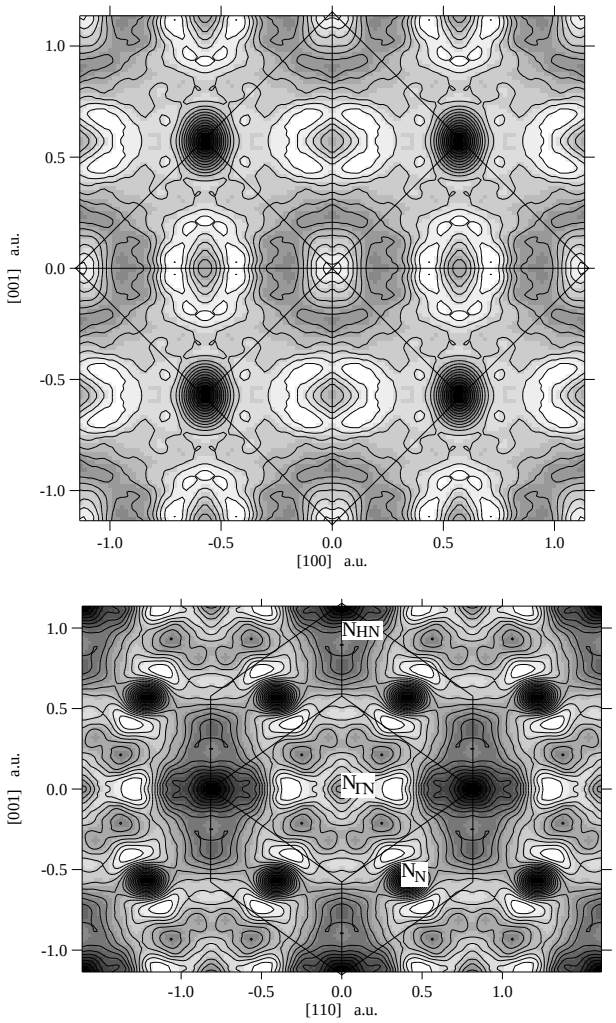

Figure 5. The maximum-entropy filtered LCW distribution of Cr: [100] (top) and [110] experimental projections.

entropy filtering technique, suggests that the Fermi surface of Cr is similar to that of Mo, but that something is perturbing the measurement in Cr. Given that the Cr data need to be 'filtered' to reveal what is probably the true FS topology (similar to that of Mo), possible explanations must be addressed. The effect of the different temperatures of the Cr (353 K) and Mo (∼30 K) samples would be twofold. Firstly, the resolution FWHM at 353 K would be expected to be about twice that at 30 K. This would indeed degrade the resolution of the Cr experiment, but experiments performed on Mo at room temperature still generate the same FS topology. Secondly, there is the consequence of the Debye–Waller factors reducing the contribution of the higher-momentum components (owing to the lattice vibrations 'reducing' the periodicity). This cannot be responsible, since the Debye temperature of Cr is so high (∼460 K). It is tempting to ascribe the perturbations present in the raw Cr LCW distributions to positron wavefunction effects. However, then the possible reasons for the greater positron perturbations in Cr (compared to Mo) have to be addressed.

Since the integration direction [110] is common to the Cr and Mo projections in figures 2 and 3, an interpretation in terms of directional behaviour (as in [4]) would require the positron wavefunction 'cosines' to have much larger amplitudes in Cr. Another possibility is the existence of disordered local moments in Cr above T_N, and the effect that these might have on the electronic structure. For the time being, this question remains unanswered.

4. Conclusions

In the light of the fact that the unexpected differences in the 2D-ACAR LCW-folded densities representing the FS topologies of Cr and Mo can be removed by maximum-entropy filtering, it is suggested that the FS topologies are indeed similar, and that the differences should be ascribed to a perturbation of the electronic structure in Cr. The question of the stronger positron effects in Cr (compared to Mo) remains unanswered, as does that of any possible effect of the magnetism. Compton scattering experiments, which are free from any positron perturbations, designed to address this question are under way.

Acknowledgments

The authors would like to thank the EPSRC, the Royal Society and Royal Commission for the Exhibition of 1851 (UK) for generous financial support, and A A Manuel for useful discussions and making his data available. One of us (SBD) would in addition like to thank the Swiss National Science Foundation.

References

[1] Fawcett E, Alberts H L, Galkin V Y, Noakes D R and Yahkmi J V 1994 *Rev. Mod. Phys.* **66** 25
[2] West R N 1995 *Proc. Int. Enrico Fermi School of Physics: Positron Spectroscopy of Solids* ed A Dupasquier and A P Mills Jr (Amsterdam: IOS Press) p 75
[3] Lock D G, Crisp V H C and West R N 1973 *J. Phys. F: Met. Phys.* **3** 561
[4] Lock D G and West R N 1975 *Appl. Phys.* **6** 249
[5] Haghighi H, Kaiser J H, Rayner S, West R N, Liu J Z, Shelton R, Howell R H, Solal F, Sterne P A and Fluss M J 1991 *J. Phys. Chem. Solids* **52** 1535
[6] Biasini M, Alam M A, Harima H, Onuki Y, Fretwell H M and West R N 1994 *J. Phys.: Condens. Matter* **6** 7823
[7] Dugdale S B, Alam M A, Fretwell H M, Biasini M and Wilson D 1994 *J. Phys.: Condens. Matter* **6** L435
[8] Hoffmann L, Shukla A, Peter M, Barbiellini B and Manuel A A 1993 *Nucl. Instrum. Methods* A **335** 276
[9] O'Brien K M, Brand M Z, Rayner S and West R N 1995 *J. Phys.: Condens. Matter* **7** 925
[10] Mattheiss L F 1965 *Phys. Rev.* **139** A1893
[11] Wood J H 1962 *Phys. Rev.* **126** 1693
[12] Kaiser J H, Walters P A, Bull C R, Alam A, West R N and Shiotani N 1987 *J. Phys. F: Met. Phys.* **17** 1243
[13] Bull C R, Alam A, West R N, Shiotani N, Singh A K and Singru R M 1983 *Positron Annihilation* ed P C Jain, R M Singru and K P Gopinathan (Singapore: World Scientific) p 266
[14] Matsumoto M and Wakoh S 1986 *J. Phys. Soc. Japan* **55** 3948
[15] Sundararajan V, Kanhere D G and Singru R M 1992 *J. Phys.: Condens. Matter* **4** 8975
[16] Singh A K, Manuel A A and Walker E 1988 *Europhys. Lett.* **6** 67
[17] See, e.g.,
Gull S F and Skilling J 1985 *Maximum Entropy and Bayesian Methods in Inverse Problems* ed C R Smith and W T Grandy Jr (Dordrecht: Reidel)
[18] West R N, Mayers J and Walters P A 1981 *J. Phys. E: Sci. Instrum.* **14** 478
[19] Andersen O K 1975 *Phys. Rev.* B **12** 3060
Jarlborg T and Arbman G 1977 *J. Phys. F: Met. Phys.* **7** 1635
Jarlborg T and Singh A K 1985 *J. Phys. F: Met. Phys.* **15** 727